EXCESS NUMBERS OF ENHANCED CPR CRATERS IN THE LUNAR POLAR REGIONS. B. J. Thomson[1,2], D. B. J. Bussey[2], J. T. S. Cahill[2], C. D. Neish[2], R. Kirk[3], G. W. Patterson[2], R. K. Raney[2], and P. D. Spudis[3], [1]Boston Univ. Center for Remote Sensing, Boston MA 02215 (bjt@bu.edu), [2]JHU Applied Physics Lab, Laurel MD 20723, [3]US Geological Survey, Flagstaff AZ, [4]Lunar and Planetary Institute, Houston TX 77058.

Summary: Mini-RF data of craters in permanent shadow near the lunar poles are consistent with a modeled ice-regolith mixture that contains upwards of 5 wt% H_2O ice, although this model is non-unique – similar polarization signatures due to roughness alone are difficult to rule out. Yet the relative abundance of craters with an "anomalous" polarization signature (initially reported by [1]) that are consistent with roughness or modest ice fractions is greater in the polar regions compared to the equator by a ratio of ~1.6:1, suggesting that roughness alone is not responsible for the polarization signature of polar craters, at least not in all cases.

Background: Numerous lines of evidence suggest modest concentrations of volatile species, including OH^- and H_2O, are present in the lunar polar regions [2-6]. Radar is an optimal instrument for detecting thick (i.e., multiple wavelengths) deposits of water ice [e.g., 7] in regions of permanent shadow as radar provides its own illuminaton source. Here we report on observations of the polarization signature of polar craters made by the Lunar Reconnaissance Orbiter's (LRO's) Mini-RF instrument and compare the relative abundance of these craters in the south polar region to their abundance in an equatorial region.

Mini-RF characteristics: Mini-RF is a dual-band, synthetic aperture radar (SAR) onboard LRO operating primarily in the S-band (2.38 GHz, 12.6 cm wavelength) [8, 9]. To date, Mini-RF has collected S-band zoom mode data (15 m resolution) for approximately 66% of the lunar surface, including >99% of the area poleward of 80 degrees N and S latitude [10].

Observations: As observed by Mini-RF radar data, the majority of impact craters >8 km in diameter in the polar regions contain modest enhancements of circular polarization ratio (CPR) in their interiors (mean CPR values ~0.8 to 1.5; Fig. 1). Examples include Shackleton crater near the lunar south pole [11]. South polar craters with similar CPR enhancements to Shackleton include Laveran (11.5 km in diameter, centered at 81.7°S, 199.5°E,), Ibn Bajja (11.3 km in diameter, centered at 86.3°S, 285.5°E), an unnamed crater in Wiechert (10.9 km in diameter, centered at 84.5°S, 161.1°E), and Braude crater (9.9 km in diameter, centered at 81.8°S, 158.3°E). In each of these cases, the radar reveals a modest enhancement in CPR in the interior of the crater only. This is in contrast to fresh impact craters, where enhanced CPR is found both inside and outside of the crater rim and is presumably attributable to rough-textured, fresh impact ejecta. Not all regions that contain permanent shadow, however, contain enhanced CPR. Mini-RF observations of the LCROSS impactor site indicate CPR values comparable to or less than the average for the south polar region [12].

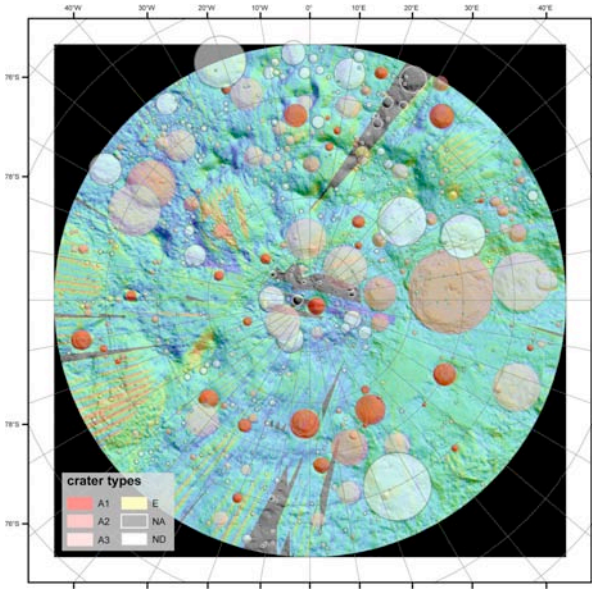

Figure 1. South polar craters classified using Mini-RF colorized CPR (circular polarization ratio) data overlain on LOLA shaded relief topography. Craters larger than 1 km have been classified as anomalous (A1-A3), fresh (E; exterior and interior enhancement), non-distinct from background (ND), or no available Mini-RF data (NA). Categoy A1 includes craters with a strong CPR enhancement over the full interior; category A2 includes moderate and/or partial interior CPR enhancements; and A3 includes low and/or patchy interior enhancements.

Synthetic SAR model: The interior CPR enhancements of Shackleton and other polar craters are consistent with a modeled ice-regolith mixture that contains ~5-10% H_2O ice, although this model is non-unique. This model is predicated on a physical mixture where the ice fraction is concentrated into wavelength or larger-sized pieces [13], such as ice cobbles larger than several 10's of cm across. Although radar is a good discriminator between thick, massive ice deposits (at least several radar wavelengths in thickness) and diffuse scattering due to surface and near-surface bur-

ied roughness elements (i.e., rocks), there is little distinction between the polarization signatures of modest ice fractions and moderately rough surfaces [14], particularly when the ice is present as small, disseminated particles in a silicate regolith. Therefore, although this CPR signature of polar craters is potentially attributable to ice, the effects of roughness alone cannot be ruled out. (However, ongoing work using diffuse scatter models [15] may help resolve this ambiguity.) This is demonstrated by Mini-RF observations of some equatorial craters that also exhibit modest CPR enhancements in their interiors only (a finding consistent with previous observations [16]). Since these equatorial craters are exposed to full sunlight over the course of a lunar day, their temperature range is incompatible with the long-term accumulation and preservation of ice deposits. Rather, their observed radar characteristics are presumably due to them being relatively recent craters (Copernican/Late Eratosthenian) in which subsequent modification has muted the exterior ejecta but not high-slope areas of the crater walls.

Abundance of anomalous craters: Despite the inability of Mini-RF monostatic data to readily distinguish between craters that contain a small amount of ice and those with moderately rough interiors, an additional piece of information about these craters is provided by their relative abundance. Examination of non-polar craters in the nearside equatorial region between 0-30°N and 0-30°W (Fig. 2) indicate that for craters in the 8 to 100 km diameter range, craters with interior CPR enhancements (hereafter termed "anomalous" craters following the nomenclature of *Spudis et al.* [1]) occupy <45% of the total crater population (Fig 3b). In the polar regions, the situation is dramatically different. Here, the majority of the craters (>70%) 8-100 km in diameter are anomalous (Fig. 3). The excess of anomalous craters above the baseline equatorial case suggests that roughness alone is not responsible for the polarization signature of polar craters, at least not in all cases. Since this difference is greater than (and in the opposite direction from) proposed polar/equatorial cratering rate differences [e.g., 17], the most plausible explanation is that the excess number of anomalous polar craters is due to the presence of accumulated ice deposits.

Future work: A planned campaign of bistatic observations using ground signals transmitted from the Arecibo radio telescope and received lunar surface echoes using Mini-RF should be better able to determine which candidate polar craters contain ice and which are merely rough.

References: [1] Spudis P.D. et al. (2010) *GRL*, *37*, L06204. [2] Feldman W.C. et al. (2001) *JGR*, *106*, 23231-23252. [3] Elphic R.C. et al. (2007) *GRL*, *34*, 13204. [4] Mitrofanov I.G. et al. (2010) *Science*, *330*, 483-486. [5] Pieters C.M. et al. (2009) *Science*, *326*, 568-572. [6] Colaprete A. et al. (2010) *Science*, *330*, 463-468. [7] Ostro S.J. (1993) *Rev. Mod. Phys.*, *65*, 1235-1279. [8] Raney R.K. (2007) *IEEE Trans. GRS*, *45*, 3397-3404. [9] Nozette S. et al. (2010) *Space Sci. Rev.*, *150*, 285-302. [10] Bussey D.B.J. et al. (2011) *LPSC*, *42*, abstract #2086. [11] Thomson B.J. et al. (2011) *LPSC*, *42*, abstract #1626. [12] Neish C.D. et al. (2011) *JGR*, *116*, E01005. [13] Lichtenberg C.L., (2000), Ph.D. thesis, Johns Hopkins Univ. [14] Thompson T.W. et al. (2011) *JGR*, *116*, E01006. [15] Thompson T.W. et al. (2012) *LPSC*, *43*, this vol. [16] Stacy N.J.S. et al. (1997) *Science*, *276*, 1527-1530. [17] Gallant J. et al. (2009) *Icarus*, *202*, 371-382.

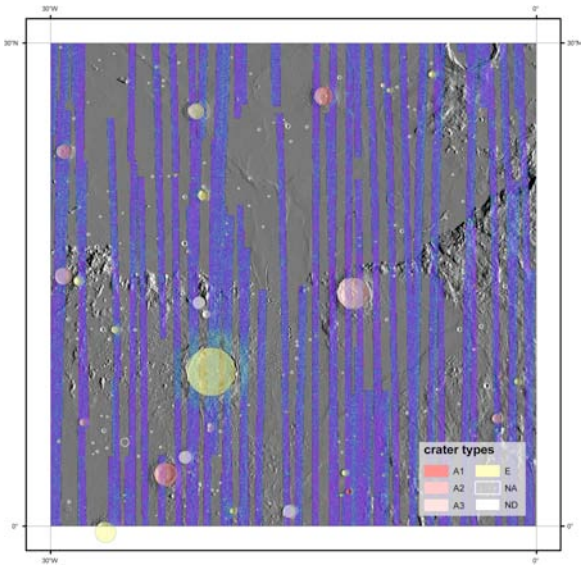

Figure 2. Equatorial craters (0-30°N, 0-30°W) classified using Mini-RF colorized CPR (circular polarization ratio) data overlain on LOLA shaded relief topography. Craters larger than 1 km have been classified in an identical manner to Fig. 1.

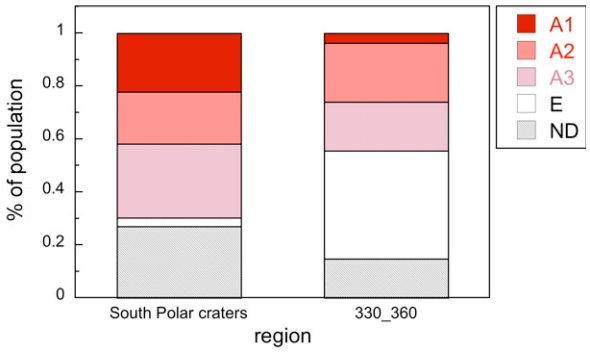

Figure 3. Bar plot of the craters 8-100 km in diameter classified in the south polar region (left) and in the equatorial study area (right). Areas in red are subclasses of anomalous craters identified in Figs. 1 & 2.